

# Gyral Folding Pattern Analysis via Surface Profiling

Kaiming Li<sup>1,2</sup>, Lei Guo<sup>1</sup>, Gang Li<sup>1</sup>, Jingxin Nie<sup>1</sup>, Carlos Faraco<sup>3</sup>, Qun Zhao<sup>4</sup>,  
Stephen Miller<sup>3</sup>, and Tianming Liu<sup>2</sup>

<sup>1</sup> School of Automation, Northwestern Polytechnical University, Xi'an, China

<sup>2</sup> Department of Computer Science, The University of Georgia, Athens, GA, USA

<sup>3</sup> Department of Psychology, The University of Georgia, Athens, GA, USA

<sup>4</sup> Department of Physics and Astronomy, The University of Georgia, Athens, GA, USA  
likaiming@gmail.com

**Abstract.** Human cortical folding pattern has been studied for decades. This paper proposes a gyrus scale folding pattern analysis technique via cortical surface profiling. Firstly, we sample the cortical surface into 2D profiles and model them using power function. This step provides both the flexibility of representing arbitrary shape by profiling and the compactness of representing shape by parametric modeling. Secondly, based on the estimated model parameters, we extract affine-invariant features on the cortical surface and apply the affinity propagation clustering algorithm to parcellate the cortex into regions with different shape patterns. Finally, a second-round surface profiling is performed on the parcellated cortical regions, and the number of hinges is detected to describe the gyral folding pattern. Experiments demonstrate that our method could successfully classify human gyri into 2-hinge, 3-hinge and 4-hinge gyri. The proposed method has the potential to significantly contribute to automatic segmentation and recognition of cortical gyri.

## 1 Introduction

The cerebral cortex of human brain is highly convoluted and folds itself into gyri and sulci during brain development. As an essential characteristic of geometry of human cerebral cortex, the folding, however, has shown quite variable patterns on even major gyri and sulci across subjects [1]. Though the mechanisms of cortical folding are still largely unknown [2], evidence has shown that the folding pattern of human cerebral cortex may predict its function [3]. Recently, the quantitative description of folding patterns has emerged as an important research goal [4-6].

The folding pattern of cerebral cortex is a multi-scale concept whose research scope can vary from a very small neighborhood to a whole brain cortical surface (Fig. 1). Currently, there are two major streams of cortical folding pattern analysis. One is based on the very local descriptor curvature and its derivations and whose scope is usually a small neighborhood that is one ring away from the focused vertex (Fig. 1a). In contrast, the other main stream is a quite global one. These latter studies use gyrification index [4] or spherical wavelets [5] to analyze the folding pattern of the whole cortical surface, or at least a certain lobe of human brain (Figs. 1e and 1f). Both techniques have been studied for decades, and have generated many successful applications [7-8]. However, neither of them represents the cortical folding pattern comprehensively and systematically, since

essentially cortical folding is a multi-scale concept. One would get quite different descriptions if he/she focused on different scales for the same cortical surface.

This paper proposes a method to analyze the folding pattern of gyri via surface profiling. This is a hybrid parametric method and profiling method in the sense that it combines both advantages of a parametric method (achieving compact representation of shape) and a profiling method (achieving flexibility of arbitrary shape representation). The basic idea is to represent 3D shape information of cortical surface patches with modeling parameters of a series of 2D profiles, and to cluster the cortex into regions with this shape information. Then a second round surface profiling is performed on the gyrus crown of the parcellated cortex, and the number of hinges is detected to describe the folding pattern of the gyrus (please see Fig. 3c for the definitions of a gyrus crown and a hinge). With surface profiling on gyri crowns, we can extend cortical folding analyses from localized parametric representations to gyrus-scale representations.

**Fig. 1.** Multi-scale description of cortical folding patterns. (a): micro-scale (red area, described by curvature); (b): meso-scale (yellow area, described by polynomial model or Bezier surface model); (c): gyrus scale (blue patch, our method); (d): sulcus scale (by [9]); (e): lobe scale (by gyrification index [4]); (f): global scale (by spherical wavelets [5]).

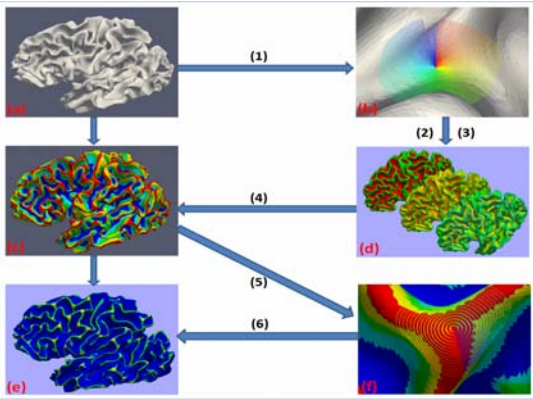
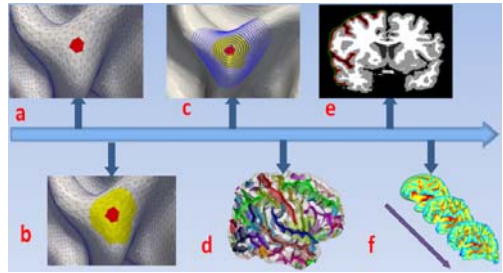


**Fig. 2.** Flowchart of our surface profiling method. (a): Original cortical surface; (b): Profiles on the original cortical surface; (c): Parcellated cortical surface; (d): Feature surfaces with shape information; (e): Gyral folding pattern surface; (f): Profiles on parcellated cortical surface. (1): Profiling; (2): Model fitting; (3): Feature extraction; (4): Affinity propagation clustering; (5): Profiling; (6): Hinge detection.

## 2 Method

### 2.1 Overview of the Method

As shown in Fig. 2, our method for gyral folding pattern analysis includes the following steps. Firstly, for each vertex of a reconstructed human brain inner surface, we sample the corresponding patch into a series of 2D profiles, and model these profiles using power function, which is a popular model in structural geology study [12]. The shape information of the current surface patch then is encoded in the parameters of the power function.

Secondly, based on the model parameters and profiling information, we define several affine-invariant features to represent each vertex's folding information, and use these features to cluster the whole cortical surface by the affinity propagation algorithm; this step segments the surface into several major cortical regions, including gyri crowns. Finally, a second round profiling is applied for vertices of gyri crowns on the parcellated cortex, and the number of hinges for each gyrus is detected to represent its folding pattern.

## 2.2 Profiling of the Cortical Surface

To profile the cortical surface, we first build a 3D coordinate system that combines a 3D Cartesian coordinate system [13] and a 2D polar coordinate system. For any vertex  $O$  on the cortical surface, we use its normal direction  $N$  as the  $Z$  direction in a 3D Cartesian coordinate system, and build a polar coordinate system in its tangent plane  $P$ . Then, we start profiling from an arbitrary direction in plane  $P$ , and stop profiling for current direction when samples reach a certain maximum  $M$ . Profiling is performed every  $\theta$  degree in plane  $P$ . Fig. 3 is an example of profiling.

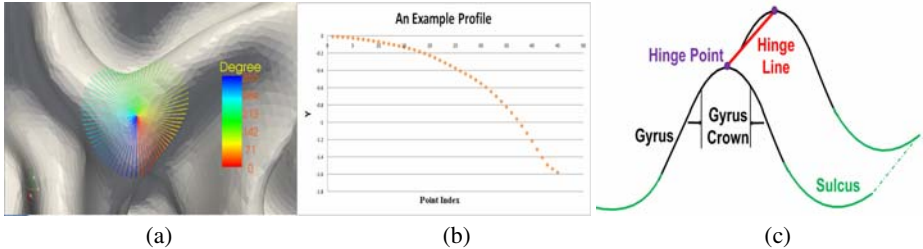


**Fig. 3.** (a) and (b): An example of profiling. (c): Definition of a gyrus crown and a hinge.

The essence of surface profiling here is to simplify a 3D profiling problem down to a collection of 2D profiling problems. This simplification is founded on the fact that the human brain is highly convoluted and surface patches can have very complex shapes. However, current popular models for 3D shapes like polynomials and ellipsoids are symmetric or might be too simple to capture such complex shapes. Thus, the advantage of 2D profiling is the flexibility to describe an arbitrarily shaped cortical surface patch. The disadvantage along with the simplification is the possible loss of 3D shape information. However, the 360 degrees of profiling still captures a great deal of 3D information, especially when we model the profiles and connect corresponding model parameters of all profiles together to form a circle curve.

## 2.3 Model Fitting

The essential idea of model fitting for profiles is to encode the shape information into a couple of parameters compactly. The model we use in this paper is the power function, a popular model in 2D Geology study because of its simplicity and intrinsic physical meaning [12]. The power function is expressed as:

$$y = y_0 \left( x / x_0 \right)^n \quad (1)$$

Here,  $x_0$ ,  $y_0$  and  $n$  are parameters to describe a profile shape;  $y_0 \neq 0$ ,  $x_0 > 0$  and  $n > 0$ . The parameters of this model can be evaluated in a sense of least-square using the Levenberg-Marquardt algorithm. Given  $N$  sample points of a profile, the parameters are those that minimize the fitting residuals:

$$\hat{P} = \arg \min_P \sum_{i=1}^N (y_i - y_{pi})^2 \quad (2)$$

Here,  $P$  denotes the three parameters to be evaluated,  $y_{pi}$  is the model output at the  $i$ -th point with  $P$  given, and  $y_i$  is the profile measurement at the  $i$ -th point.

## 2.4 Feature Extraction and Clustering

After the model fitting step, we extract several affine-invariant features to represent the shape information of a surface patch. Among the model parameters, the ratio  $R$  between  $y_0$  and  $x_0$  and the power  $n$  are very information-rich descriptors of the profile shape, especially the ratio  $R$  which has proven to be more stable and changes more smoothly between adjacent profiles than the power  $n$ . The definitions and descriptions of features that we extract based on model parameters and profiling information are as follows. 1) SulciOrGyri: a vertex that has more profile points above its tangent plane would be considered as on a sulcus. Otherwise, it is on a gyrus. 2) AverRatio: the average  $R$  of all profiles for the current vertex. 3) AverMinR: average of  $R$ s that correspond to local minimums at  $R$  curve. 4) AverMaxR: average of  $R$ s that correspond to local maximums at  $R$  curve. 5) AllDis: sum of distances between neighboring local maximum and minimum. 6) AverDis: average of distances between neighboring local maximum and minimum. 7) MaxDis: maximum of distances between neighboring local maximum and minimum. 8) AverSampleDis: average of the first order moment of all profiles about the tangent plane. 9) MaxSampleDis: maximum of the first order moment of all profiles about the tangent plane. 10) AverPower: average of the power  $n$  for all profiles.

Based on the above 10 features, we apply the unsupervised clustering algorithm affinity propagation [14] to the vertices of a cortical surface. The similarity  $S(i, j)$  of two random vertices  $i$  and  $j$  is defined as the minus weighted Mahalanobis distance:

$$S(i, j) = -\sqrt{(\bar{V}_i - \bar{V}_j)^T Cov^{-1} W (\bar{V}_i - \bar{V}_j)} \quad (3)$$

Here  $\bar{V}_i$  and  $\bar{V}_j$  are the feature vector defined above;  $W$  is a weighting diagonal matrix with  $W_{ii}$  as the weight for the  $i$ -th feature;  $Cov$  is the feature covariance.

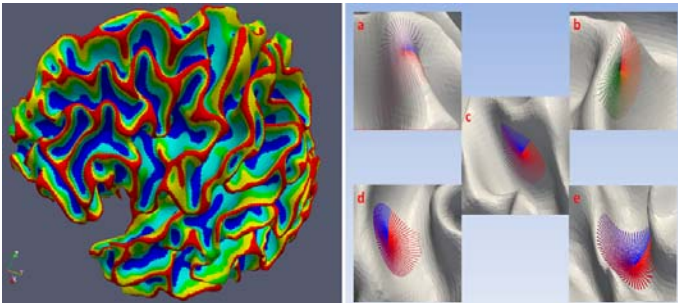


**Fig. 4.** The five parcelated cortical regions and their typical corresponding patches: gyrus crown (red, a), sub gyrus crown (yellow, b), central area (green, c), sub sulcus basin (light blue, d), and sulcus basin (blue, e)

An example of the clustering result is shown in Fig. 4. The clustering step has two important contributions. First, the cortical surface is automatically parcellated into distinct regions corresponding to gyral and sulcal regions, as well as transitional regions between them. Second, the transition between different cortical regions is smooth. If we walk from gyrus crown to sulcus basin along any path, we will very likely cross the same three transitional cortical regions. These two properties significantly help us profile the gyrus crown on the parcellated cortex and analyze gyral folding patterns.

## 2.5 Profiling on Gyrus Crown and Hinge Detection

To profile the gyrus crown of the parcellated cortex, we first assign a label to each parcellated cortical region. The assigned labels could reflect the layout and transition between different cortical regions. In this paper, gyri crowns are assigned with a value 1 whereas sulci basins are assigned with a value 5, and other regions are assigned with values according to their transitional levels on the parcellated cortex.

Then, a feature  $f$  is created for each profile of gyrus crown in order to measure the profile depth, as well as the number of different regions the profile crosses. The feature is defined as:

$$f = \frac{1}{N} \sum_{i=1}^N f_i \quad (4)$$

Here  $N$  is the number of points on the profile, and  $f_i$  is the label of the region to which point  $i$  belongs. For example, if point  $i$  is on the gyrus crown,  $f_i$  is 1.

Following the above two steps, we detect hinges of the gyrus on which the current vertex sits. After 360 degree profiling, the feature values of all profiles for the current vertex will be combined together to form a ring curve (see Fig. 5d). Local minima of the curve correspond to the hinges of the gyrus, and the number of the local minima is the number of hinges of the gyrus. For example, vertex A in Fig 5 has a very clear folding pattern (three local minima) to indicate that it is on a 3-hinge gyrus.

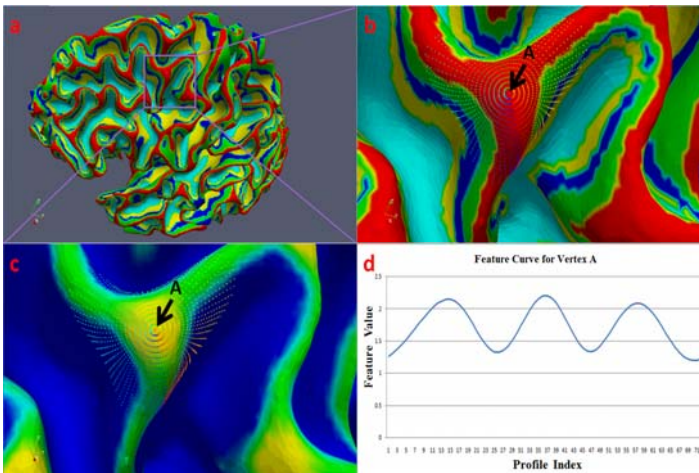


**Fig. 5.** Profiling of a gyrus crown on parcellated cortex. (a): the parcellated cortex; (b): profiling on a gyrus crown; (c): detected patterns (yellow for 3-hinge gyri, and green for 2-hinge gyri); (d): the feature curve for vertex A.

### 3 Results

#### 3.1 Gyri Pattern Detection

In this section, we applied the above method to 10 constructed cortical surfaces. Our experimental results demonstrate that human gyral folding patterns can be divided into 3 classes according to their number of hinges: 2-hinge, 3-hinge and 4-hinge gyri. Fig. 6a shows examples of the three folding pattern categories and Fig. 6b shows their corresponding feature curves respectively. As we can see from the figure, the hinges of gyri correspond well to the local minima of the feature curves (Fig. 6b). The number of local minima of the connected feature curve, therefore, is considered as the number of hinges for the current gyrus. Besides the number of local minima of the connected feature curve, the distance between local minima is also an important feature that could be used to further classify the detected gyral folding patterns. This distance actually represents the degree of how much the gyrus bends itself. Take the 2-hinge gyrus in Fig. 6a3 as an example, its bending degree is apparently larger than Fig. 6a1 and Fig. 6a2 in the same category. We can also see the differences from the feature curves in Fig. 6b, that is, the distance of the two local minima in Fig. 6b3 is larger than those of the other two gyri in Fig. 6b1 and Fig. 6b2.

Fig. 6c provides the gyri pattern detection result on a whole cortical surface. Apparently, most of the gyri patterns are correctly detected, indicating reasonably good performance of the proposed method. In particular, the detected 4-hinge patterns are highlighted by dashed circles. One zoomed example is shown in Fig. 6d.

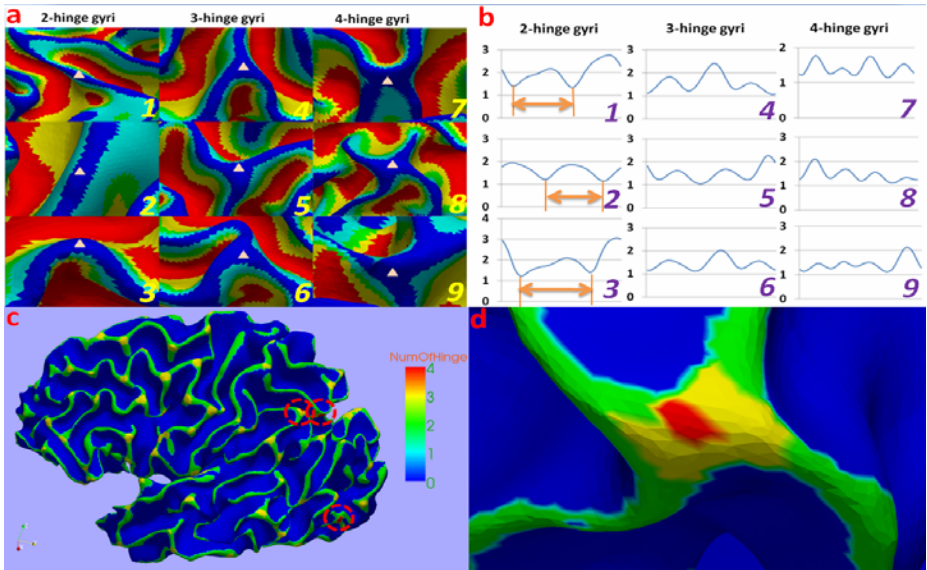


**Fig. 6.** Pattern detection result. (a): Examples for each detected pattern. Small triangles denote the centers of detected gyri patterns. 1-3: 2-hinge gyri; 4-6: 3-hinge gyri; 7-9: 4-hinge gyri. (b): Corresponding feature curve for each sample. (c): Detected patterns on a whole cortical surface. The three patterns are color-coded. (d): An example of detected 4-hinge gyri.

### 3.2 Accuracy

To quantitatively evaluate the accuracy of our proposed method, we have two experts manually label the detected patterns, and count the number of two types of detection errors: Type1 error (false positive) and Type2 error (false negative). We express the accuracy as:

$$DetectionAccuracy = (1 - \frac{Type1Errors + Type2Errors}{AllDetectedPatterns}) * 100\% \quad (5)$$

The detection accuracy of the 3-hinge gyri pattern for the randomly selected 10 cortical surfaces is summarized in Table 1. The average accuracy is over 90%. The algorithm has similar accuracy performance for the 2-hinge and 4-hinge gyri pattern detections.

**Table 1.** Detection accuracy for 3-hinge gyri pattern

Subject ID	Expert 1		Expert 2		Detected Patterns	Accuracy (%)
	Error1	Error2	Error1	Error2		
Sub 1	8	6	7	5	184	92.93
Sub 2	5	9	6	11	196	92.09
Sub 3	6	4	8	3	170	93.82
Sub 4	4	11	4	9	143	90.21
Sub 5	10	9	9	9	168	88.98
Sub 6	6	4	6	5	181	94.19
Sub 7	1	8	3	9	146	92.80
Sub 8	9	3	7	3	203	94.58
Sub 9	10	11	8	10	154	87.34
Sub 10	7	3	5	5	165	93.93
Total	58	70	63	69	1410	90.78

## 4 Discussion and Conclusion

In this paper, we propose a method to analyze gyral folding pattern via surface profiling. The method focuses on hinge numbers of gyri, and has been applied to 10 normal human brain MR images. Our preliminary results demonstrate that the proposed surface profiling method is able to accurately classify gyri into three folding patterns according to the number of gyral hinges.

In the extant literature, several methods have been proposed to automatically label human brain surface into gyri and sulci [10-11]. In comparison, our segmentation of the cortical surface is based on clustering using profile shape information, and 3 more classes besides gyrus crown and sulcus basin are segmented to fill the transition area from gyri to sulci. Though the segmented gyrus crown might be broken somewhere, it seems that these breaks have little impact on the final results of gyral folding patterns. This robustness may come from the profiling method itself. Since we profile the cortical surface at a macro level, small breaks of a gyrus crown probably would not change the fact that the majority of the profile is on a gyrus.

Our research on gyral folding pattern analysis has shown that 3-hinge and 4-hinge gyri (Fig. 6d) are common across different subjects, and the distribution of them among individuals can vary significantly. This result puts forward new challenges for registration-based analysis of the human brain. For example, how to establish correspondence between different patterns of gyri, e.g., 3-hinge gyri and 4-hinge gyri, in brain registration remains a challenging and open problem.

Currently, our method only classifies gyral folding patterns into 3 broad classes: 2-hinge, 3-hinge, and 4-hinge gyri. A more detailed classification of the folding patterns, however, is possible via surface profiling. For the 2-hinge gyri, we could use the angle between local minima to recognize whether it is a “-” shape gyrus or “U” shape gyrus. For the three-hinge gyri, we could also use the angle information to further classify the gyri into “Y” shapes and “T” shapes. The more detailed classification of 2-hinge gyri and 3-hinge gyri could potentially provide additional important features for self-contained parcellation of the cerebral cortex into anatomically meaningful regions, as well as for automatic recognition of them.

## References

1. Talairach, J., Tournoux, P.: *Co-planar Stereotaxic Atlas of the Human Brain*. Thieme, New York (1988)
2. Van Essen, D.: A tension-based theory of morphogenesis and compact wiring in the central nervous system. *Nature* 385, 313–318 (1997)
3. Fischl, B., Rajendran, N., Busa, E., et al.: Cortical Folding Patterns and Predicting Cytoarchitecture. *Cereb Cortex* 18(8), 1973–1980 (2008)
4. Zilles, K., Armstrong, E., Schleicher, A., Kretschmann, H.J.: The human pattern of gyrification in the cerebral cortex. *Anat. Embryol. (Berl)* 179, 173–179 (1988)
5. Yu, P., Grant, P.E., Qi, Y., Han, X., et al.: Cortical Surface Shape Analysis Based on Spherical Wavelets. *IEEE Transaction on Medical Imaging* 26(4), 582–597 (2007)
6. Toro, R., Perron, M., Pike, B., et al.: Brain Size and Folding of the Human Cerebral Cortex. *Cerebral Cortex* 18(10), 2352–2357 (2008)
7. Hardan, A.Y., Jou, R.J., Keshavan, M.S., et al.: Increased frontal cortical folding in autism: a preliminary MRI study. *Psychiatry Research: Neuroimaging* 131, 263–268 (2004)
8. Rettmann, M.E., Kraut, M.A., Prince, J.L., et al.: Cross-sectional and longitudinal analyses of anatomical sulcal changes associated with aging. *Cerebral Cortex* 16, 1584–1594 (2006)
9. Mangin, J.F., Rivière, D., Cachia, A., et al.: A framework to study the cortical folding patterns. *NeuroImage* 23, S129–S138 (2004)
10. Cachia, A., Mangin, J.F., Rivière, D., et al.: A generic framework for parcellation of the cortical surface into gyri using geodesic Voronoi diagrams. *Med. Image. Anal.* 7(4), 403–416 (2003)
11. Fischl, B., van der Kouwe, A., Destrieux, C., et al.: Automatically parcellating the human cerebral cortex. *Cereb. Cortex.* 14(1), 11–22 (2004)
12. Bastida, F., Aller, J., Bobillo-Ares, N.C.: Geometrical analysis of folded surfaces using simple functions. *Journal of structural geology* 21, 729–742 (1999)
13. Tao, X., Prince, J.L., Davatzikos, C., et al.: Using a Statistical Shape Model to Extract Sulcal Curves on the Outer Cortex of the Human Brain. *IEEE Trans. Med. Imag.* 21(5), 513–524 (2002)
14. Frey, B.J., Dueck, D.: Clustering by Passing Messages Between Data Points. *Science* 315, 972–976 (2006)